## Title
Rescue of a primary myelofibrosis model by retinoid-antagonist therapy



## Journal
Proceedings of the National Academy of Sciences of the United States of America, 110(47)

## ISSN
0027-8424

## Authors
Hong, Suk-Hyun
Dvorak-Ewell, Melita
Stevens, Hazel Y
et al.

## Publication Date
2013-11-19

## DOI
10.1073/pnas.1318974110

Peer reviewed

# Rescue of a primary myelofibrosis model by retinoid-antagonist therapy

Suk-Hyun Hong[a], Melita Dvorak-Ewell[b], Hazel Y. Stevens[c,1], Grant D. Barish[a], Glenda L. Castro[a], Russell Nofsinger[a,2], John A. Frangos[c], Dolores Shoback[b], and Ronald M. Evans[a,d,3]

[a]Gene Expression Laboratory, Salk Institute for Biological Studies, La Jolla, CA 92037; [b]Endocrine Research Unit, Department of Veterans Affairs Medical Center, University of California, San Francisco, CA 94121; [c]La Jolla Bioengineering Institute, San Diego, CA 92121; and [d]Howard Hughes Medical Institute, Salk Institute for Biological Studies, La Jolla, CA 92037

Contributed by Ronald M. Evans, October 11, 2013 (sent for review September 20, 2013)

**Molecular targeting of the two receptor interaction domains of the epigenetic repressor silencing mediator of retinoid and thyroid hormone receptors (SMRT$^{mRID}$) produced a transplantable skeletal syndrome that reduced radial bone growth, increased numbers of bone-resorbing periosteal osteoclasts, and increased bone fracture risk. Furthermore, SMRT$^{mRID}$ mice develop spontaneous primary myelofibrosis, a chronic, usually idiopathic disorder characterized by progressive bone marrow fibrosis. Frequently linked to polycythemia vera and chronic myeloid leukemia, myelofibrosis displays high patient morbidity and mortality, and current treatment is mostly palliative. To decipher the etiology of this disease, we identified the thrombopoietin (*Tpo*) gene as a target of the SMRT–retinoic acid receptor signaling pathway in bone marrow stromal cells. Chronic induction of *Tpo* in SMRT$^{mRID}$ mice results in up-regulation of TGF-β and PDGF in megakaryocytes, uncontrolled proliferation of bone marrow reticular cells, and fibrosis of the marrow compartment. Of therapeutic relevance, we show that this syndrome can be rescued by retinoid antagonists, demonstrating that the physical interface between SMRT and retinoic acid receptor can be a potential therapeutic target to block primary myelofibrosis disease progression.**

splenomegaly | ostesclerosis | myelodysplastic syndrome

Bone is a dynamic tissue maintained by an intricate balance of two key components, osteoclasts and osteoblasts (1). Osteoclasts, which originate from hematopoietic progenitors in the marrow compartment, continuously resorb bone matrix, whereas osteoblasts, which originate from the mesenchymal progenitors, deposit new matrix (2). Imbalance between these two activities leads to either loss of the bone matrix in osteoporosis or excessive accumulation of the matrix in osteopetrosis (3). Thus, the basis of pathogenic conditions in either compartment can be traced back to the microenvironments created by opposing mesenchymal and hematopoietic lineages (4, 5).

Myelofibrosis was characterized in 1951 by Dameshek (6) as a myeloproliferative condition manifesting as a type of chronic leukemia. In the case of idiopathic myelofibrosis, fibrotic tissue occupies the bone marrow spaces, eliminating the microenvironments and destabilizing normal hematopoiesis and bone remodeling (7). Although primary myelofibrosis appears with splenomegaly and bone pain, it commonly manifests a blood picture suggestive of polycythemia vera or chronic myeloid leukemia with reduced (often nucleated) red blood cells and increased immature white cells. The one known treatment is allogeneic stem cell transplantation, but this approach involves significant risks (8). Other treatment options are largely supportive and do not alter the course of the disorder (9). Recently the US Food and Drug Administration approved ruxolitinib (a JAK 1/2 inhibitor), supporting a view that transcriptional activation may be at the core of the disease (10, 11).

Nuclear hormone receptor (NR) signaling plays critical roles in vertebrate development, physiology, and homeostasis, and chromosomal translocation of promyelocytic leukemia (*PML*) and promyelocytic leukemia zinc finger (*PLZF*) with the retinoic acid receptor (RAR) has been shown to promote myeloid leukemia (12). Although many NR signaling pathways directly impact bone remodeling and/or hematopoietic development by controlling key cell types in each segment (13), their dependency on specific cofactors such as silencing mediator of retinoid and thyroid hormone (SMRT) or nuclear receptor corepressor is unclear at best. As bifunctional transcription factors, nonliganded NRs use corepressors to promote transcriptional silencing, a process that is relieved upon addition of ligand (14–17). To explore the corepressor functions of NRs in vivo, we generated mice carrying knock-in mutations in the two receptor interaction domains (mRID) of SMRT to produce SMRT$^{mRID}$ mice (18). Unexpectedly, SMRT$^{mRID}$ mice develop spontaneous primary myelofibrosis, a syndrome generally considered therapeutically intractable.

## Results

**Reduced Bone Radial Growth in SMRT$^{mRID}$.** A salient feature of the SMRT$^{mRID}$ bone phenotype is the dramatic reduction in radial growth without any significant differences in length, as measured by μCT (computerized tomography) and faxitron X-ray analysis (Fig. 1 *A* and *B* and Fig. S1*A*). Reduced radial growth is accompanied by cortical thinning without significant differences in cortical bone density, as revealed by peripheral quantitative CT analysis (Fig. 1*B* and Fig. S1*A*). Consistent with these defects, a ~20% reduction in fracture load is seen in SMRT$^{mRID}$ mice when subjected to a femoral neck fracture assay (Fig. 1*C*). Higher serum concentrations of the osteoclast-specific tartrate-resistant acid

### Significance

**Our work identifies a therapeutically tractable yet previously unrecognized repressive epigenetic feature of primary myelofibrosis that controls a key cytokine circuit in the bone marrow microenvironment. Though lacking previous clinical utility, we show that an orally active retinoic acid receptor antagonist can normalize thrombopoietin production, restore bone integrity, and dramatically reduce fibrosis. This identification of a pathway-specific drug for primary myelofibrosis opens up an avenue of treatment options and provides insight into the complex mechanisms underlying myelofibrosis.**

Author contributions: S.-H.H., M.D.-E., H.Y.S., J.A.F., D.S., and R.M.E. designed research; S.-H.H., M.D.-E., H.Y.S., G.D.B., and G.L.C. performed research; S.-H.H., M.D.-E., H.Y.S., and R.N. contributed new reagents/analytic tools; S.-H.H., M.D.-E., and H.Y.S. analyzed data; and S.-H.H. and R.M.E. wrote the paper.

The authors declare no conflict of interest.

Freely available online through the PNAS open access option.

[1]Present address: George W. Woodruff School of Mechanical Engineering, Atlanta, GA 30332-0405.

[2]Present address: WaferGen BioSystems, Fremont, CA 94555.

[3]To whom correspondence should be addressed. E-mail: evans@salk.edu.

This article contains supporting information online at www.pnas.org/lookup/suppl/doi:10.1073/pnas.1318974110/-/DCSupplemental.

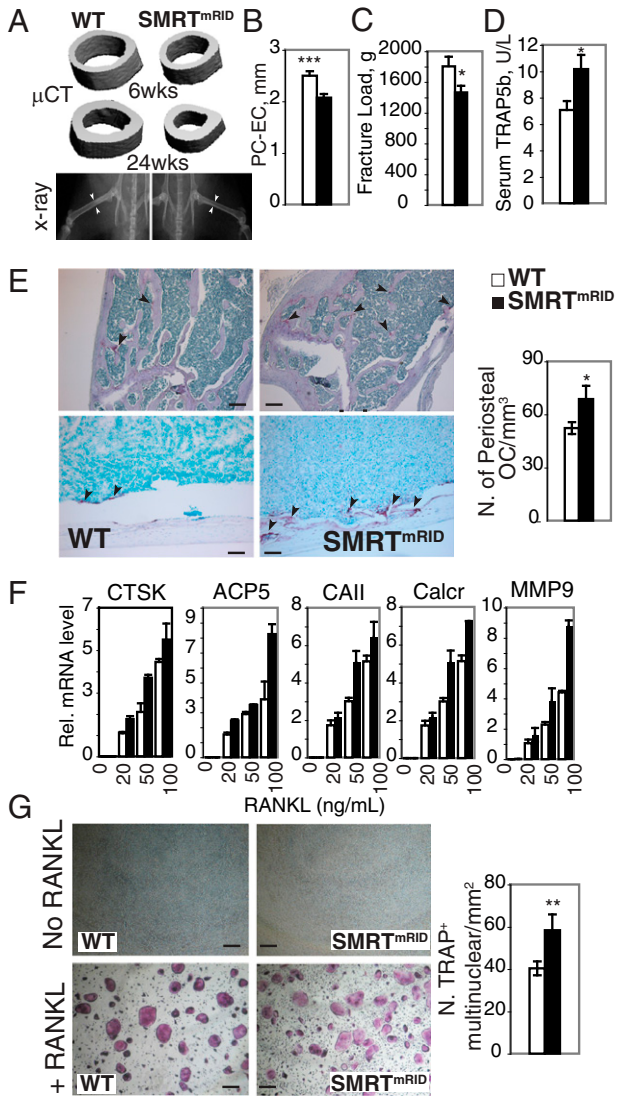


**Fig. 1.** Defective bone growth in SMRT$^{mRID}$ mice. (*A*) Comparison of radial growth in femoral midshafts using μCT (*Top*, 6-wk-old mice; *Middle*, 6-mo-old mice) and faxitron X-ray analyses (*Bottom*, arrows indicate differences in shaft thickness). (*B*) Quantitative comparison of femoral radial growth. PC, periosteal circumference; EC, endosteal circumference; PC-EC cortical bone thickness (6-mo-old mice, $n = 5$ per group). (*C*) Femoral bone fracture load (6-mo-old mice, $n = 5$ per group). (*D*) Serum levels of bone resorption marker TRAP5b (6-mo-old mice, $n = 7$ per group). (*E*) TRAP staining in femur (*Upper*) and under the periosteal surface (*Lower*) and quantitation. (Scale bars, 100 μm.) (*F*) Expression of osteoclast (OC) markers at given doses of RANKL in bone marrow in vitro. (*G*) Formation of multinuclear osteoclast-like cells with and without RANKL treatment. (Scale bars, 20 μm.) The data are shown as the mean ± SEM. $*P < 0.05$, $**P < 0.005$, $***P < 0.005$ by Student *t* test.

phosphatase (TRAP5b) in SMRT$^{mRID}$ mice suggest that the bone defects are mainly due to increased osteoclast activity (Fig. 1*D* and Fig. S1*B*). Indeed, a ~25% increase in overall osteoclast numbers is revealed by TRAP staining, whereas osteoblast activity is not significantly affected (Fig. 1*E*, *Upper*, and Fig. S1*C*). Notably, there are increased numbers of osteoclasts along the endosteal surface, consistent with the observed cortical bone thinning in SMRT$^{mRID}$ mice (Fig. 1*E*, *Lower*). Next we examined whether the increased osteoclast activity in SMRT$^{mRID}$ animals is due to enhanced sensitivity of progenitors to receptor activator of nuclear factor kappa-B ligand (RANKL). In an in vitro differentiation assay, the RANKL dose-dependently increased the expression of osteoclast markers and yielded more TRAP$^+$ multinucleated cells from SMRT$^{mRID}$ bone marrow, suggesting increased osteoclast differentiation potential (Fig. 1 *F* and *G*).

**Primary Myelofibrosis and Splenomegaly in SMRT$^{mRID}$ Mice by Age 8 Mo.** By 8 mo of age, ~30% of SMRT$^{mRID}$ mice display symptoms of splenomegaly, osteosclerosis, myelofibrosis (discussed below), and hind limb paresis (Movie S1). As the pale color of the bone suggests, extramedullary hematopoiesis is evident in the enlarged spleen and the increased numbers of megakaryocytes and erythroid progenitors seen in the SMRT$^{mRID}$ mice (Fig. 2 *A*–*C*). Analogous to the human disease state, a dramatic increase in splenic hematopoietic progenitors and a simultaneous decrease of progenitors in the bone marrow compartment is observed in SMRT$^{mRID}$ mice by colony formation assays (Fig. 2*D*). These findings, combined with the relatively normal blood count and smear profiles (Fig. S2*A*), are consistent with a hyperproliferative preleukemic state similar to polycythemia vera.

The decrease in progenitors in the bone marrow compartment is accompanied by an increase in nonhematopoietic cells in SMRT$^{mRID}$ mice (Fig. 2*E*). Histologic stains in mutant mice reveal that much of the marrow cavity is occupied by reticular cells and collagen fibers (reticulin) as typically seen in myelofibrosis patients (Fig. 2 *E* and *F*). The osteosclerosis and microvessel formation found in patients is reflected in 8-mo-old SMRT$^{mRID}$ mice whose bone marrow cavities contain large amounts of small spicules and increased numbers of CD34$^+$ microvessels (19, 20) (Fig. 2*E*). Subsequent μCT scan analysis revealed increased bone volume in trabecular regions, with a simultaneous decrease in trabecular bone spacing and increase in trabecular bone numbers, confirming the above histologic findings (Fig. 2*G* and Fig. S2*C*). Furthermore, quantitative RT-PCR from tibial samples demonstrated an increase in gene expression of osteoblast markers in conjunction with fibrogenic collagens (Fig. 2*H* and Fig. S2*B*). These changes of osteoblastic parameters are only seen after the onset of myelofibrosis in SMRT$^{mRID}$ mice.

**Thrombopoietin Overproduction and Disruption of Bone Marrow Microenvironment.** Increased cytokine gene expression is seen in SMRT$^{mRID}$ tibias, particularly thrombopoietin (*Tpo*) and TGF-β1 (Fig. 3*A*), genes previously shown to cause myelofibrosis in transgenic mouse models (21, 22). The observed increase in *Tpo* expression correlated with higher levels of circulating thrombopoietin (TPO) in the SMRT$^{mRID}$ mice (Fig. 3*B*). Furthermore, an approximate 100% increase in levels of TPO were found in the SMRT$^{mRID}$ bone marrow (Fig. 3*B*), consistent with expression of *Tpo* in stem cell compartments including bone marrow stromal cell (BMSC) (23). These findings suggest that locally produced TPO is driving megakaryocytic proliferation, which in turn precipitates and fosters the fibrotic response.

Growing evidence suggests an intricate network of cellular interactions between megakaryocytes and cells of mesenchymal lineage (23). In exploring the source of megakaryopoiesis in the fibrotic SMRT$^{mRID}$ marrow, WT mononuclear cells were cocultured on primary bone marrow stroma derived from SMRT$^{mRID}$ mice. This interaction alone was sufficient to produce a dramatic twofold increase in the numbers of CD41$^+$ megakaryocytic lineage cells, identifying an activated stromal compartment as the key cellular target of SMRT dysregulation (Fig. 3*C*).

As predicted from coculture studies, transplantation of SMRT$^{mRID}$ marrow confirmed that increased TPO production, osteosclerosis, and splenomegaly were all transferable to irradiated WT recipient mice (Fig. 3 *D*–*F* and Fig. S3*B*). Repopulation of SMRT$^{mRID}$ BMSC was established by PCR genotyping (Fig. S3*A*), and reticulin staining verified the existence of fibrosis in the recipient marrow (Fig. 3*G*).

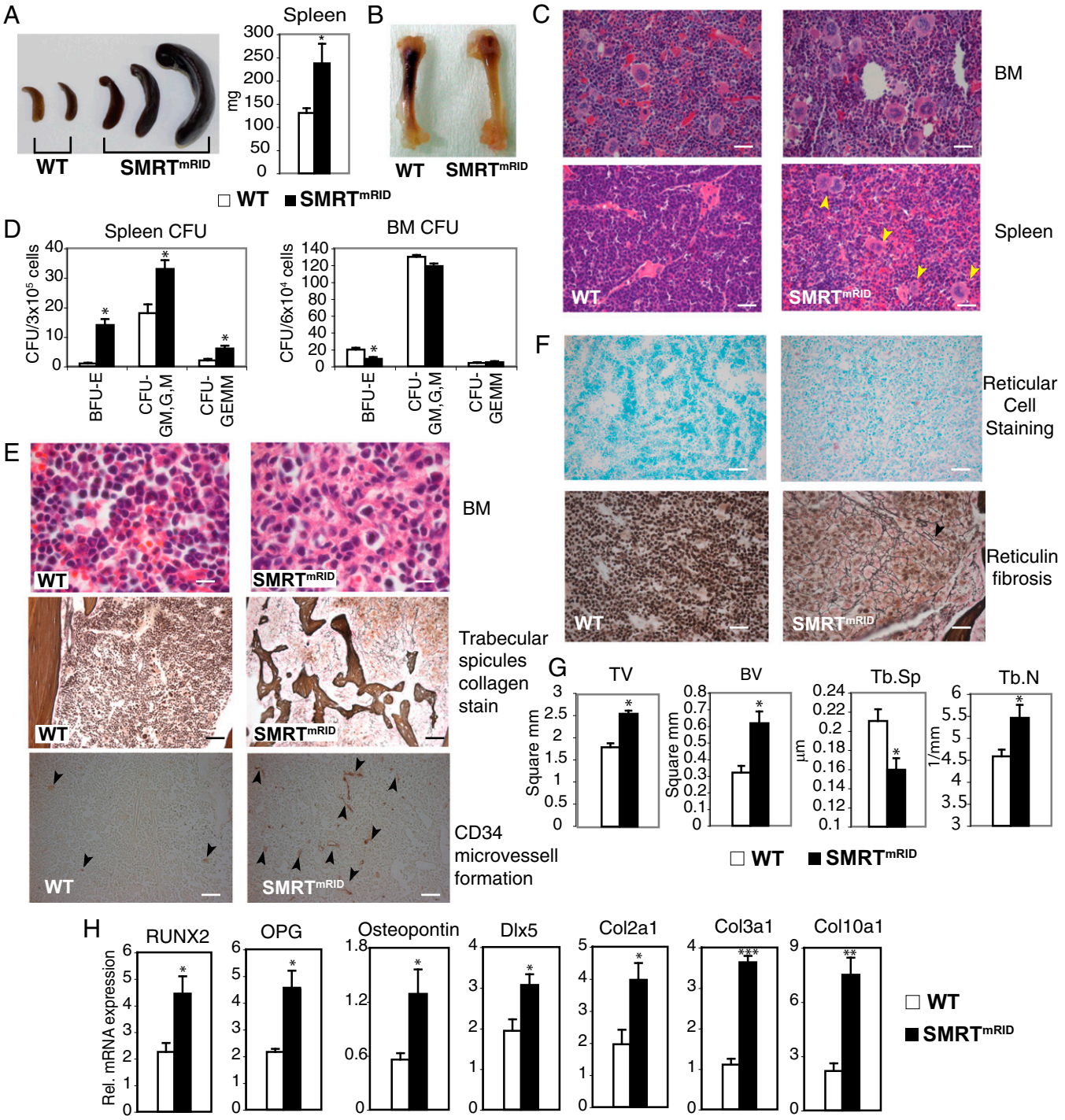


**Fig. 2.** Splenomegaly and primary myelofibrosis in SMRT$^{mRID}$ mice. (*A*) Spleens (8-mo-old mice, $n = 13$, $P < 0.05$) and (*B*) bones from WT and SMRT$^{mRID}$ mice. (*C*) Megakaryocytes in bone marrow (BM) and spleen (arrowheads) revealed by H&E staining. (Scale bar, 20 μm.) (*D*) Colony forming progenitors in the spleen in methylcellulose colony assay ($n = 5$ per group; BFU-E, erythroid burst forming unit, CFU-GM, G, M, colony-forming unit granulocyte and macrophage, granulocyte, or macrophage; CFU-GEMM, myeloid colony-forming unit). (*E*) Bone marrow histology showing nonhematopoietic nuclei and extracellular matrix by H&E staining (*Top*), small trabeculae formation in fibrotic marrow by silver staining (*Middle*), and microvessel formation by CD34 immunostaining (*Bottom*). (Scale bars, 20 μm at *Top*, 100 μm at *Middle* and *Bottom*). (*F*) Acid phosphatase staining of bone marrow sections showing pink-stained reticular cells, which are not present in WT marrow (*Upper*) and reticulin fibrosis (*Lower*). (Scale bars, 100 μm.) (*G*) Trabecular bone parameters tissue volume (TV), bone volume (BV), trabecular bone spacing (Tb.Sp), and trabecular bone number (Tb.N) measured by μCT. (*H*) Expression of osteoblast gene markers in isolated tibia. The data are shown as the mean ± SEM. $^*P < 0.05$, $^{**}P < 0.005$, $^{***}P < 0.005$ by Student *t* test.

**Loss of RAR-SMRT$^{mRID}$ Interaction Results in TPO Derepression.** Although SMRT has been reported to interact with more than a dozen transcription factors, the SMRT$^{mRID}$ mutation disables only NR-mediated repression. Consequently, we examined the upstream region of the *Tpo* promoter for potential NR binding sites. Bioinformatic analysis identified a highly conserved 200-bp

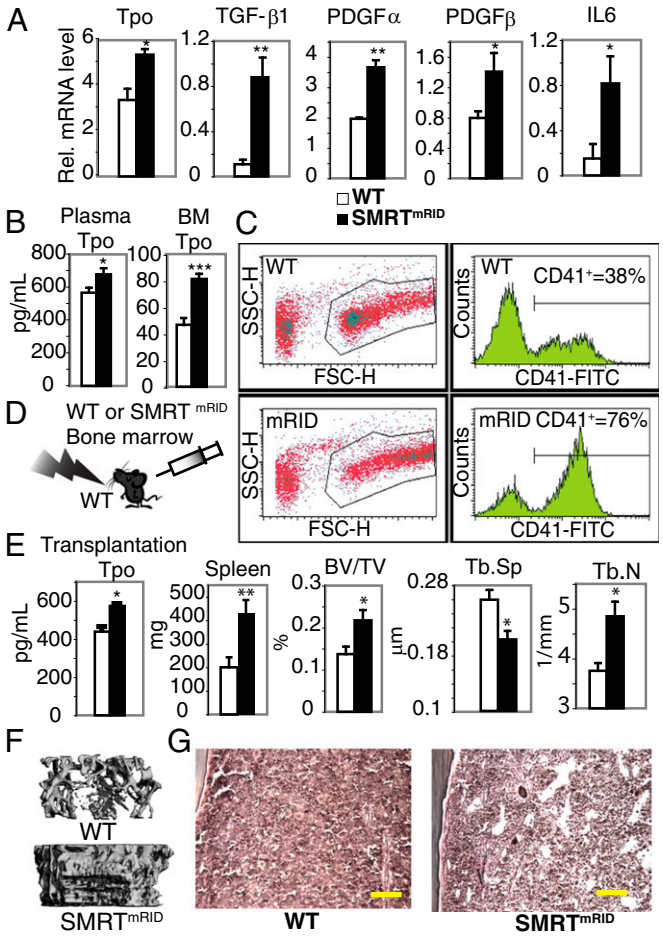


**Fig. 3.** Increased TPO and disrupted bone marrow microenvironment in SMRT$^{mRID}$ mice. (*A*) Cytokine expression in SMRT$^{mRID}$ tibias. (*B*) TPO levels in plasma and flushed bone marrow supernatants. (*C*) Flow cytometry analysis of megakaryopoiesis in BMSC feeder layers. (*D*) Cartoon of bone marrow transplantation experiment. Transplanation experiments were replicated twice. (*E*) TPO levels, spleen weight, and trabecular bone parameters in bone marrow transplant recipients. (*F*) Reconstructed μCT images of trabecular bones in transplant recipients. (*G*) Reticulin staining of transplanted bone marrow sections. (Scale bars, 100 μm.) The data are shown as the mean ± SEM. $*P < 0.05$, $**P < 0.005$, $***P < 0.005$ by Student *t* test.

region in 22 eutherian mammals (Fig. S4). Within that region, we found canonical tandem retinoic acid response elements (RAREs), consisting of direct repeats separated by 5 base pairs (DR-5) and overlapping DR-2, 3 elements, with the DR-5 element conserved between mouse, human, and other mammals (24) (Fig. 4*A*). This conserved DR-5 element displayed direct and competitive RAR-retinoid X receptor (RXR) binding in EMSA that was abrogated by targeted mutations (Fig. 4*B*). Furthermore, mutated DR-5 elements were no longer able to compete for RAR-RXR binding, establishing the conserved DR-5 as a high-affinity RAR-RXR binding site in vitro (Fig. S5 *A* and *B*). Indeed, a 2-kb genomic DNA fragment spanning the *Tpo* promoter tethered to a luciferase reporter showed that this RARE was critical in conferring retinoic acid (RA) responsiveness in the presence of RARα and -γ but not with RARβ (Fig. 4*C* and Fig. S5*C*). Of note, SMRT has been shown to bind more strongly to RARα and RARγ than RARβ (25). Consistent with this assessment, we observed that endogenous *Tpo* expression was already near its maximal level in SMRT$^{mRID}$ BMSC, even in the absence of RA (Fig. 4*D*). Enhanced target gene expression was also seen with other known RAR targets, such as cellular RA binding protein 2 and transglutaminase 2, which were superinduced in SMRT$^{mRID}$ by low concentrations of RA, compared with WT BMSC (Fig. 4*D* and Fig. S5*D*). SMRT and RAR occupancy on the *Tpo* RARE was evaluated using ChIP assays. RAR occupancy on *Tpo* RAREs was not altered in either WT or SMRT$^{mRID}$ BMSCs. In SMRT$^{mRID}$ BMSC, SMRT did not bind to the *Tpo* RARE region, whereas in WT BMSC, SMRT

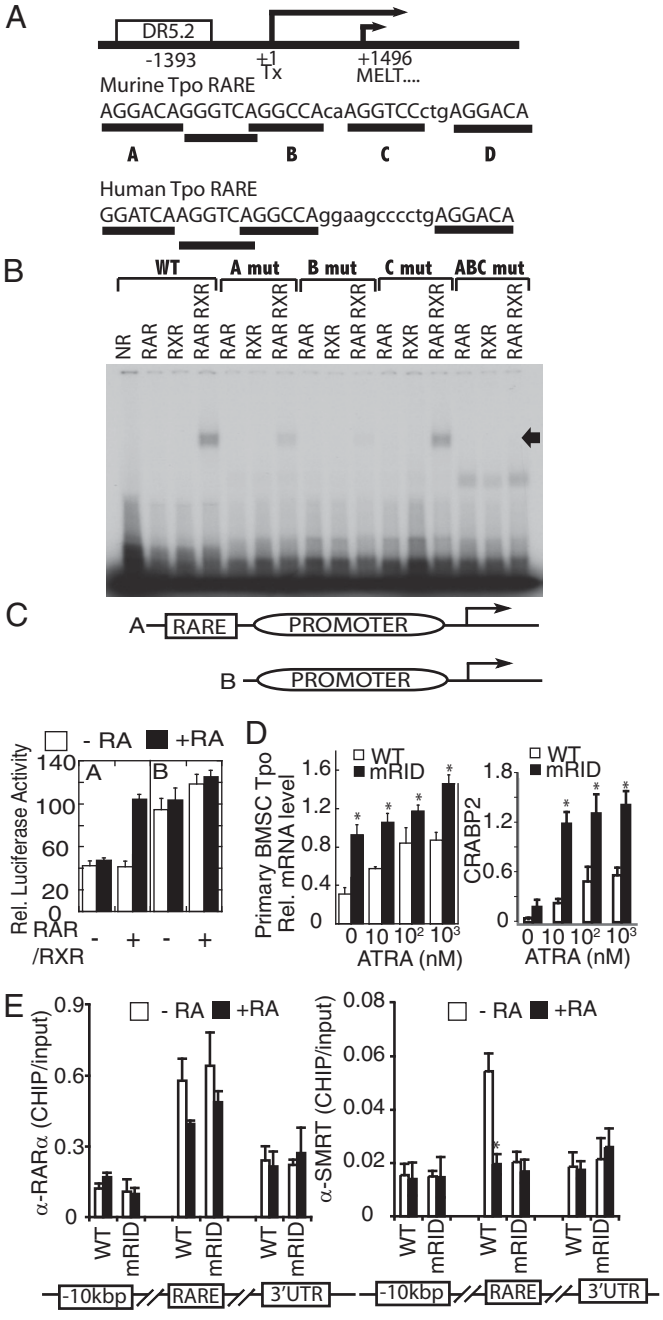


**Fig. 4.** Loss of SMRT-RAR interaction leads to thrombopoietic derepression. (*A*) Identified RAREs in murine *Tpo* promoter. (*B*) EMSA of RAR-RXR heterodimer binding to WT and mutated DR-5 RAREs. (*C*) Luciferase reporter activity of murine *Tpo* promoter in the presence or absence of the identified RARE. CV-1 cells cotransfected with empty vector or RAR and RXR treated with and without RA. (*D*) Dose-dependent expression of *Tpo* and cellular RA binding protein 2 (*Crabp2*), a known RAR target, in primary BMSC upon treatment with the RAR agonist all trans retinoic acid (ATRA). (*E*) RAR and SMRT occupancy on *Tpo* RAREs in BMSC as shown by ChIP quantitative PCR assay. The data are shown as the mean ± SEM. $*P < 0.05$ by Student *t* test.

occupancy was observed, which could be decreased by RA treatment (Fig. 4*E*). These results indicate that loss of SMRT occupancy is responsible for derepression of *Tpo* expression in BMSC.

**RAR Antagonist Treatment Normalizes Myelofibrosis in SMRT$^{mRID}$.** Furthermore, derepression of *Tpo* expression could be fully rescued by RAR antagonist in vivo, as a presumed consequence of competing with endogenous RA for receptor binding (Fig. 5 *A* and *D*). When WT or SMRT$^{mRID}$ bone marrow transplanted mice were treated with RAR antagonist for 1 mo, bone quality and myelofibrosis in SMRT$^{mRID}$ marrow transplanted mice were dramatically normalized in comparison with vehicle-treated mice (Fig. 5 *B* and *C* and Fig. S5*F*).

## Discussion

Recent molecular genetic studies have suggested that the myeloproliferative syndromes induced by loss of RARγ are due to microenvironment-driven changes in the bone marrow compartment (26). In light of our present findings, we suggest that loss of RAR leads to loss of SMRT-mediated repression, enabling uncontrolled cytokine production. We speculate that TPO transcription is mainly controlled by SMRT-RAR repressor complex, but it is possible that other corepressors such as nuclear receptor corepressor might also become involved in the presence of RAR antagonist. This idea of "RAR target derepression" is further supported by the incidence of bone marrow fibrosis in patients undergoing aggressive RA treatment during acute promyelocytic leukemia (APL) "differentiation" therapy (27). These findings suggest that the etiology of other elusive bone or hematopoietic anomalies might reside in deregulation of cytokine networks within the bone marrow microenvironment, controlled by NRs and their corepressors. Finally, our discovery that an RAR antagonist can normalize TPO production, restore bone integrity, and reduce fibrosis identifies both a unique drug and an alternative therapeutic route to potentially treat this debilitating disease.

## Materials and Methods

**Animals.** Generation and initial characterization of SMRT$^{mRID}$ mice have been described previously (18). We further backcrossed these mice for four more generations to sv129. Only age-matched male mice (average cohort size 6–10) were randomly assigned and used. All mice were bred and maintained in the Salk Institute animal facility under specific pathogen-free conditions. Procedures involving animals were reviewed and approved by the Institutional Animal Care and Use Committee at the Salk Institute and conformed to regulatory and ethical standards. Study sample sizes were based on historical efficacy data for the agents used in this study. The studies were powered to achieve statistical significance. The mouse studies were not blinded, because the same investigators performed the grouping, dosing, and analyses, rendering blinding of the studies unfeasible.

**Bone Analyses and Bone Marrow Transplantation.** See *SI Materials and Methods*.

**Gene Expression Analyses.** DNA-free total RNA was used to generate cDNA and analyzed by SYBR green-based quantitative PCR. Primers used in quantitative PCR are listed in Table S1.

**Osteoclast and Osteoblast Differentiation.** For in vitro differentiation of osteoclasts, mononuclear bone marrow cells were cultured in α-MEM supplemented with 10% (vol/vol) FBS, recombinant 50 ng/mL macrophage colony-stimulating factor, and specified amount of RANKL (Fitzgerald Industries International) for 6 d. For in vitro differentiation of osteoblast, bone marrow cells were differentiated in α-MEM containing 10% FBS, freshly added 50 mg/mL ascorbic acid, and 10 mM β-glycerophosphate for 2–3 wk.

**Serological Analyses.** Serum calcium and serum alkaline phosphatase were measured with the QuantiChrom Calcium assay kit and Alkaline Phosphatase Assay kit, respectively (BioAssay Systems). Serum TRAP5b was measured with mouse TRAP5b Assay kit (SBA Biosciences). Plasma TPO was assessed with the Mouse Thrombopoietin Quantikine ELISA Kit (R&D Systems).

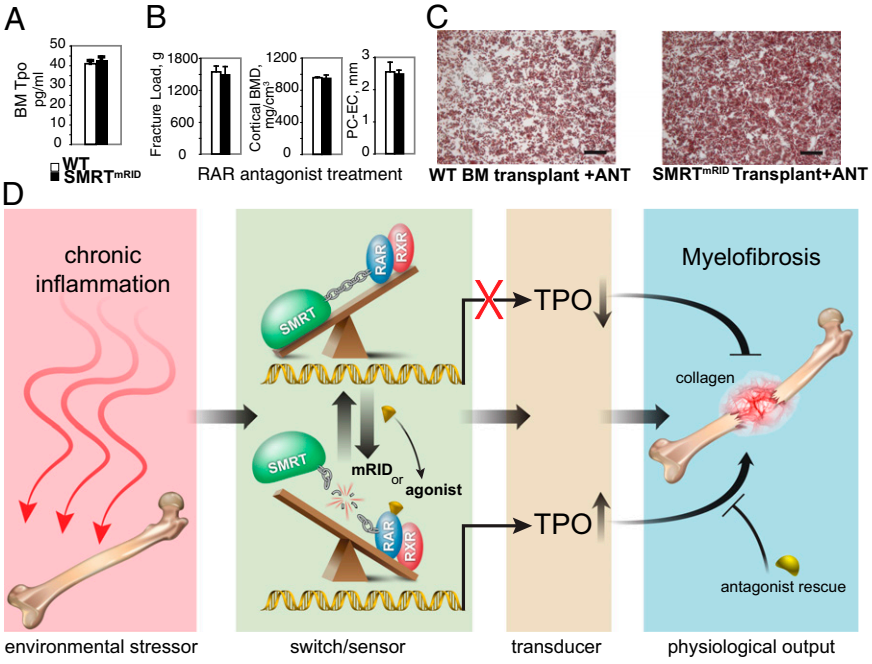


**Fig. 5.** TPO overexpression is rescued by an RAR antagonist. (*A*) TPO level in the bone marrow flush supernatant after RAR antagonist treatment (Ro 41-5253 100 mg/kg per day for 30 d, $n = 7$ per group). (*B*) Bone parameters in SMRT$^{mRID}$ mice after RAR antagonist treatment (Ro 41-5253 100 mg/kg per day for 30 d, $n = 7$ per group). (*C*) Reticulin staining of bone marrow from transplanted mice after RAR antagonist treatment (Ro 41-5253 100 mg/kg per day for 30 d). Transfection experiments were replicated three times. Transplantation and antagonist treatments were replicated twice. (Scale bars, 50 μm.) (*D*) Cartoon depicting the unique role of SMRT-mediated repression of RAR-regulated TPO expression in primary myelofibrosis. The data are shown as the mean ± SEM. *$P < 0.05$ by Student *t* test.

**Cell Culture.** CV-1 cells were obtained from ATCC (catalog no. CCL-70) and tested free of Mycoplasma contamination. Primary bone marrow stroma were isolated and cultured in Myelocult (Stemcell Technologies). For co-culture assay, irradiated (15 Gy) BMSC were cocultured with freshly isolated bone marrow cells and cultured for 2 wk. The resulting population of cells was analyzed with the LSR I flow cytometer (BD Biosciences). For colony formation assay, bone marrow cell or splenocytes were analyzed using Methocult media per the manufacturer's instructions (Stemcell Technologies).

**Promoter Analyses.** Conserved promoter regions were identified using Ensembl alignment tools (28). EMSA and luciferase reporter assays were performed as previously described (29). Briefly, CV-1 cells were transfected with the pGL3 basic luciferase reporters with various promoter fragments of mouse *Tpo* using Effectene (Qiagen). Forty-eight hours after transfection, cells were harvested, and β-galactoside and luciferase activity were determined. We performed ChIP assays with primary BMSCs following the protocols (Upstate) using RARα (catlog no. sc-551X, Santa Cruz Biotechnology) and SMRTe antibodies (catalog no. 06-891, Millipore). Primers used in ChIP assay are listed in Table S1.

**Statistics and General Methods.** Appropriate statistical analyses were applied, assuming a normal sample distribution, as specified in the figure legends. No samples were excluded from the statistical analyses because investigators were not blinded in the studies. Variances for each group data were calculated and used for Student *t* test.

**ACKNOWLEDGMENTS.** We thank Martin Privalsky (University of California, Davis) for providing the recombinant baculoviruses for RAR and RXR expression, Dzung T. Le (University of California, San Diego) for discussion on the hematological assessment, Diana Measy for technical assistance, L. Ong and C. Brondos for administrative assistance, and Ruth Yu, Annette Atkins, and Michael Downes for manuscript editing and suggestions. This work was supported by the Howard Hughes Medical Institute, the Leona M. and Harry B. Helmsley Charitable Trust, Ipsen/Biomeasure, the Glenn Foundation for Medical Research, The Samuel Waxman Cancer Research Foundation, The Ellison Medical Foundation, and National Institutes of Health grants DK057978, DK090962, HL088093, and HL105278. The Salk Core facility μCT scanner is supported by the VA Research Enhancement Award Program in Bone Disease. R.M.E. is an investigator of the Howard Hughes Medical Institute at the Salk Institute for Biological Studies and March of Dimes Chair in Molecular and Developmental Biology.

1. Karsenty G, Wagner EF (2002) Reaching a genetic and molecular understanding of skeletal development. *Dev Cell* 2(4):389–406.
2. Teitelbaum SL (2000) Bone resorption by osteoclasts. *Science* 289(5484):1504–1508.
3. Wan Y, Chong LW, Evans RM (2007) PPAR-gamma regulates osteoclastogenesis in mice. *Nat Med* 13(12):1496–1503.
4. Purton LE, Scadden DT (2006) Osteoclasts eat stem cells out of house and home. *Nat Med* 12(6):610–611.
5. Perry JM, Li L (2007) Disrupting the stem cell niche: Good seeds in bad soil. *Cell* 129(6): 1045–1047.
6. Dameshek W (1951) Some speculations on the myeloproliferative syndromes. *Blood* 6(4):372–375.
7. Abdel-Wahab OI, Levine RL (2009) Primary myelofibrosis: Update on definition, pathogenesis, and treatment. *Annu Rev Med* 60:233–245.
8. Fleischman AG, Maziarz RT (2013) Hematopoietic stem cell transplantation for myelofibrosis: Where are we now? *Curr Opin Hematol* 20(2):130–136.
9. Tefferi A (2011) How I treat myelofibrosis. *Blood* 117(13):3494–3504.
10. Mascarenhas J, Hoffman R (2013) A comprehensive review and analysis of the effect of ruxolitinib therapy on the survival of patients with myelofibrosis. *Blood* 121(24): 4832–4837.
11. Ostojic A, Vrhovac R, Verstovsek S (2011) Ruxolitinib: A new JAK1/2 inhibitor that offers promising options for treatment of myelofibrosis. *Future Oncol* 7(9):1035–1043.
12. Petrie K, Zelent A, Waxman S (2009) Differentiation therapy of acute myeloid leukemia: Past, present and future. *Curr Opin Hematol* 16(2):84–91.
13. Bland R (2000) Steroid hormone receptor expression and action in bone. *Clin Sci (Lond)* 98(2):217–240.
14. Ordentlich P, et al. (1999) Unique forms of human and mouse nuclear receptor corepressor SMRT. *Proc Natl Acad Sci USA* 96(6):2639–2644.
15. Chen JD, Evans RM (1995) A transcriptional co-repressor that interacts with nuclear hormone receptors. *Nature* 377(6548):454–457.
16. Hörlein AJ, et al. (1995) Ligand-independent repression by the thyroid hormone receptor mediated by a nuclear receptor co-repressor. *Nature* 377(6548):397–404.
17. Sande S, Privalsky ML (1996) Identification of TRACs (T3 receptor-associating cofactors), a family of cofactors that associate with, and modulate the activity of, nuclear hormone receptors. *Mol Endocrinol* 10(7):813–825.
18. Nofsinger RR, et al. (2008) SMRT repression of nuclear receptors controls the adipogenic set point and metabolic homeostasis. *Proc Natl Acad Sci USA* 105(50):20021–20026.
19. Vannucchi AM, Migliaccio AR, Paoletti F, Chagraoui H, Wendling F (2005) Pathogenesis of myelofibrosis with myeloid metaplasia: Lessons from mouse models of the disease. *Semin Oncol* 32(4):365–372.
20. Mesa RA, Hanson CA, Rajkumar SV, Schroeder G, Tefferi A (2000) Evaluation and clinical correlations of bone marrow angiogenesis in myelofibrosis with myeloid metaplasia. *Blood* 96(10):3374–3380.
21. Chagraoui H, et al. (2002) Prominent role of TGF-beta 1 in thrombopoietin-induced myelofibrosis in mice. *Blood* 100(10):3495–3503.
22. Kakumitsu H, et al. (2005) Transgenic mice overexpressing murine thrombopoietin develop myelofibrosis and osteosclerosis. *Leuk Res* 29(7):761–769.
23. Kacena MA, Gundberg CM, Horowitz MC (2006) A reciprocal regulatory interaction between megakaryocytes, bone cells, and hematopoietic stem cells. *Bone* 39(5): 978–984.
24. Kinjo K, et al. (2004) All-trans retinoic acid directly up-regulates thrombopoietin transcription in human bone marrow stromal cells. *Exp Hematol* 32(1):45–51.
25. Wong CW, Privalsky ML (1998) Transcriptional silencing is defined by isoform- and heterodimer-specific interactions between nuclear hormone receptors and corepressors. *Mol Cell Biol* 18(10):5724–5733.
26. Walkley CR, et al. (2007) A microenvironment-induced myeloproliferative syndrome caused by retinoic acid receptor gamma deficiency. *Cell* 129(6):1097–1110.
27. Hatake K, et al. (1996) Tretinoin induces bone marrow collagenous fibrosis in acute promyelocytic leukaemia: New adverse, but reversible effect. *Br J Haematol* 93(3): 646–649.
28. Flicek P, et al. (2013) Ensembl 2013. *Nucleic Acids Res* 41(Database issue):D48–D55.
29. Hong SH, Privalsky ML (2000) The SMRT corepressor is regulated by a MEK-1 kinase pathway: Inhibition of corepressor function is associated with SMRT phosphorylation and nuclear export. *Mol Cell Biol* 20(17):6612–6625.